iScience, Volume *25*

Supplemental information

Single-cell atlas

of the aging mouse colon

Dovydas Širvinskas, Omid Omrani, Jing Lu, Mahdi Rasa, Anna Krepelova, Lisa Adam, Sandra Kaeppel, Felix Sommer, and Francesco Neri

Supplementary Information

Supplementary material contains 5 Supplementary Figures

Supplementary Figures:

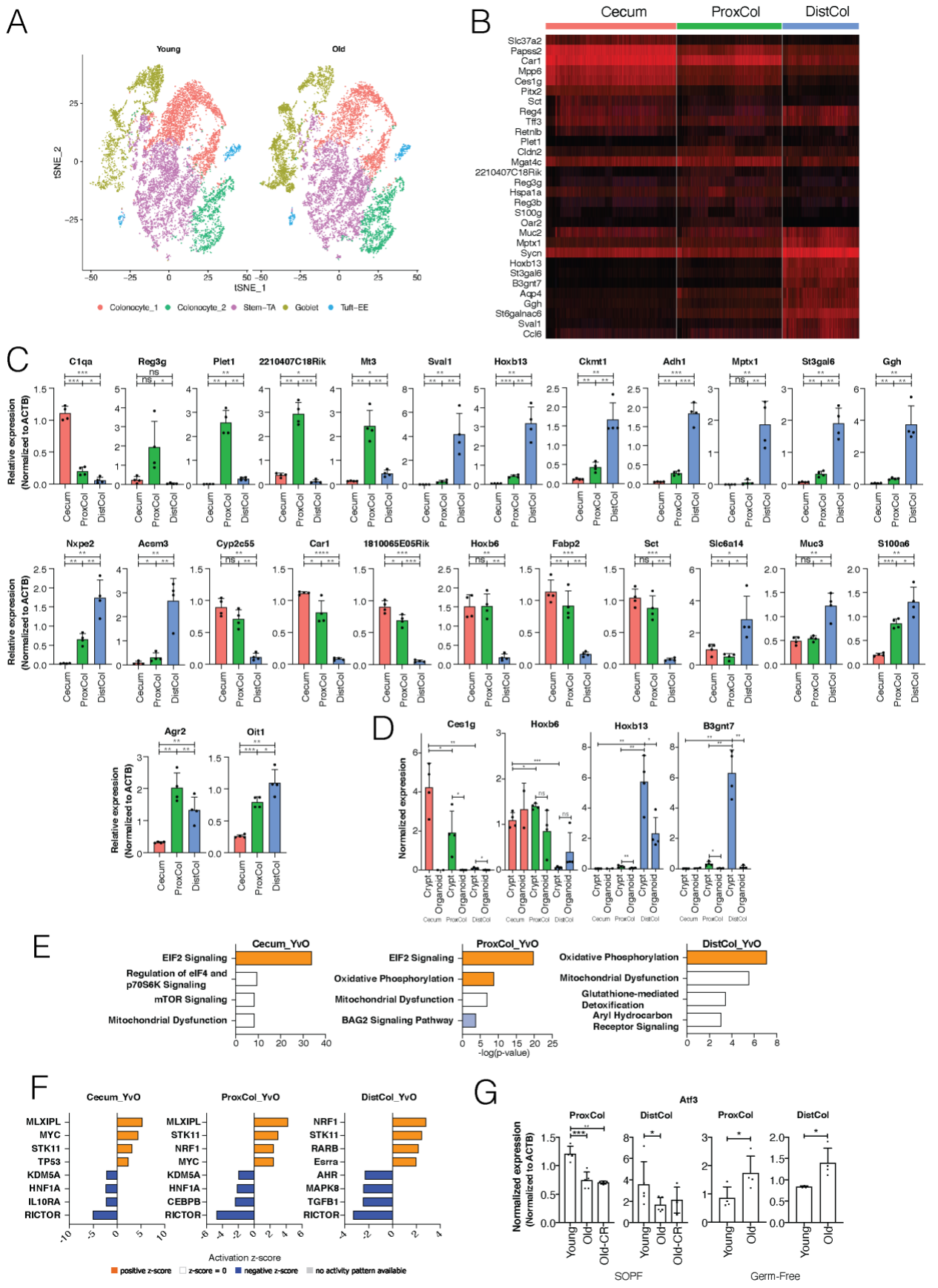
A
Young
Old
tSNE_2
tSNE_1
Colonocyte_1
Colonocyte_2
Stem−TA
Goblet
Tuft−EE
B
Cecum
ProxCol
DistCol
Slc37a2
Papss2
Car1
Mpp6
Ces1g
Pitx2
Sct
Reg4
Tff3
Retnlb
Plet1
Cldn2
Mgat4c
2210407C18Rik
Reg3g
Hspa1a
Reg3b
S100g
Oar2
Muc2
Mptx1
Sycn
Hoxb13
St3gal6
B3gnt7
Aqp4
Ggh
St6galnac6
Sval1
Ccl6
C
C1qa
Reg3g
Plet1
2210407C18Rik
Mt3
Sval1
Hoxb13
Ckmt1
Adh1
Mptx1
St3gal6
Ggh
Nxpe2
Acsm3
Cyp2c55
Car1
1810065E05Rik
Hoxb6
Fabp2
Sct
Slc6a14
Muc3
S100a6
Agr2
Oit1
Relative expression (Normalized to ACTB)
Cecum
ProxCol
DistCol
D
Ces1g
Hoxb6
Hoxb13
B3gnt7
Normalized expression
Crypt
Organoid
E
Cecum_YvO
EIF2 Signaling
Regulation of eIF4 and p70S6K Signaling
mTOR Signaling
Mitochondrial Dysfunction
ProxCol_YvO
EIF2 Signaling
Oxidative Phosphorylation
Mitochondrial Dysfunction
BAG2 Signaling Pathway
DistCol_YvO
Oxidative Phosphorylation
Mitochondrial Dysfunction
Glutathione-mediated Detoxification
Aryl Hydrocarbon Receptor Signaling
-log(p-value)
F
Cecum_YvO
MLXIPL
MYC
STK11
TP53
KDM5A
HNF1A
IL10RA
RICTOR
ProxCol_YvO
MLXIPL
STK11
NRF1
MYC
KDM5A
HNF1A
CEBPB
RICTOR
DistCol_YvO
NRF1
STK11
RARB
Esrra
AHR
MAPK8
TGFB1
RICTOR
Activation z-score
positive z-score
z-score = 0
negative z-score
no activity pattern available
G
Atf3
ProxCol
DistCol
Normalized expression (Normalized to ACTB)
Young
Old
Old-CR
SOPF
Germ-Free

Figure S1. Compartment differences of young colonic epithelium, related to Fig.1.
(A) Separated tSNE plots of young and old mice (n = 5 young, 6 old biologically independent animals) **(B)** Top 10 marker gene heatmap for large intestinal compartments. **(C)** qPCR performed on crypts isolated from different compartments of young female mice (n = 4 biologically independent animals; 1-tailed paired *t*-test; mean + SD). **(D)** qPCR performed on crypt and organoid pairs from different compartments of young male mice. (n = 4 biologically independent animals (n = 2 cecum organoid samples); 1-tailed paired *t*-test used between young compartments, 1-tailed unpaired *t*-test used between young and old animals; mean + SD). **(E)** Enriched Canonical Pathways from IPA for compartments. (n = 5 young, 6 old biologically independent animals) **(F)** Predicted Upstream Regulators from IPA for compartments. (n = 5 young, 6 old biologically independent animals) **(G)** qPCR performed on crypts isolated from different compartments of young, old and old calorie restricted specific pathogen free female mice as well as young and old germ-free female mice. (SOPF: n = 5 young, 5 old and 4 old calorie restricted biologically independent animals (Young ProxCol n = 4); Germ-Free: n = 4 young, 4 old biologically independent animals; 1-tailed unpaired *t*-test; mean + SD). ns, $p>=0.05$; *, $p<0.05$; **, $p<0.01$; ***, $p<0.001$;

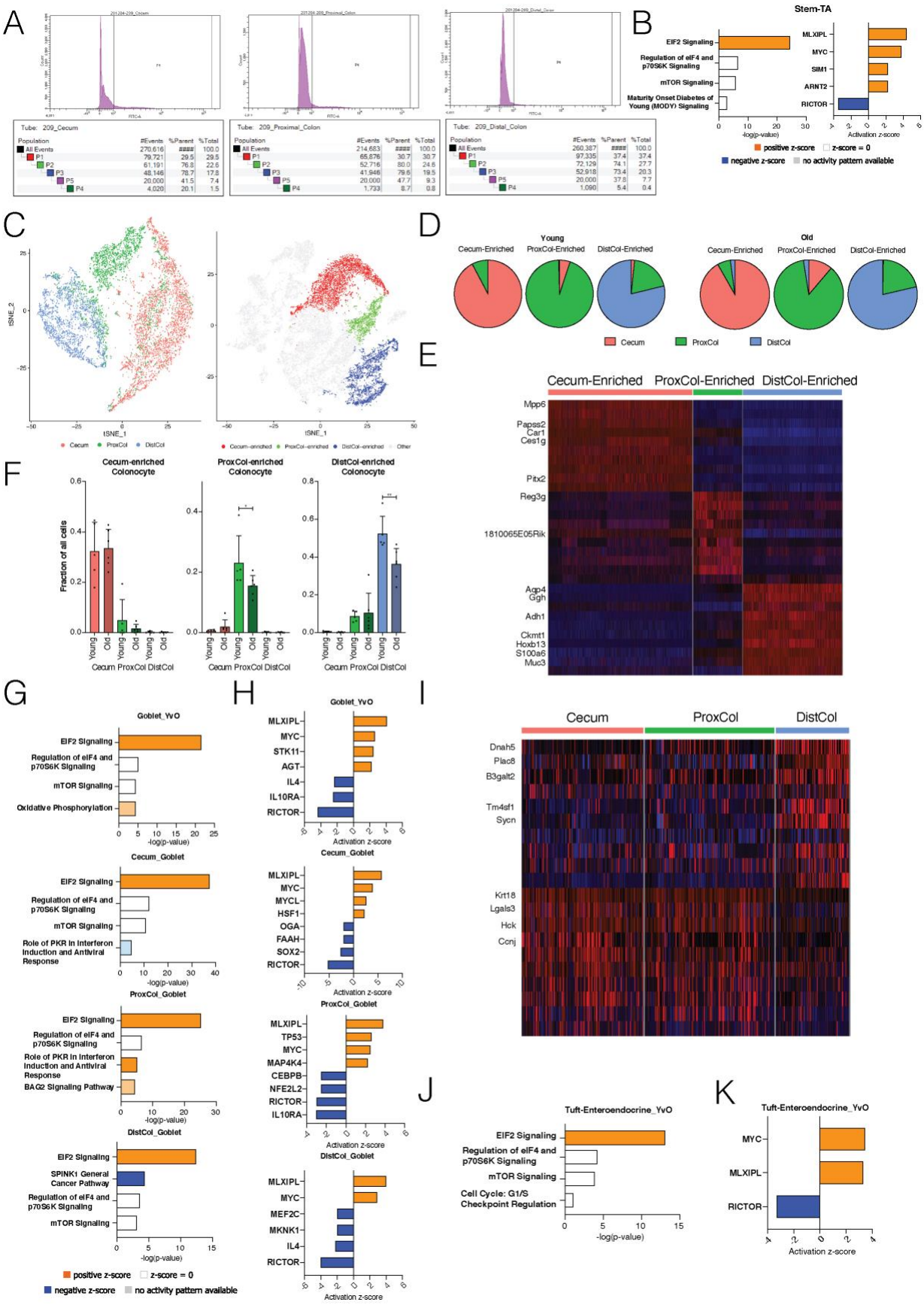
A
Tube: 209_Cecum
Population #Events %Parent %Total
All Events 270,616 #### 100.0
P1 79,721 29.5 29.5
P2 61,191 76.8 22.6
P3 48,146 78.7 17.8
P5 20,000 41.5 7.4
P4 4,020 20.1 1.5
Tube: 209_Proximal_Colon
Population #Events %Parent %Total
All Events 214,683 #### 100.0
P1 65,876 30.7 30.7
P2 52,716 80.0 24.6
P3 41,946 79.6 19.5
P5 20,000 47.7 9.3
P4 1,733 8.7 0.8
Tube: 209_Distal_Colon
Population #Events %Parent %Total
All Events 260,387 #### 100.0
P1 97,335 37.4 37.4
P2 72,129 74.1 27.7
P3 52,918 73.4 20.3
P4 1,090 5.4 0.4
B
Stem-TA
EIF2 Signaling
Regulation of eIF4 and p70S6K Signaling
mTOR Signaling
Maturity Onset Diabetes of Young (MODY) Signaling
-log(p-value)
MLXIPL
MYC
SIM1
ARNT2
RICTOR
Activation z-score
positive z-score
z-score = 0
negative z-score
no activity pattern available
C
tSNE_1
tSNE_2
Cecum
ProxCol
DistCol
Cecum-enriched
ProxCol-enriched
DistCol-enriched
Other
D
Young
Old
Cecum-Enriched
ProxCol-Enriched
DistCol-Enriched
Cecum
ProxCol
DistCol
E
Cecum-Enriched ProxCol-Enriched DistCol-Enriched
Mpp6
Papss2
Car1
Ces1g
Pitx2
Reg3g
1810065E05Rik
Agp4
Ggh
Adh1
Ckmt1
Hoxb13
S100a6
Muc3
F
Cecum-enriched Colonocyte
ProxCol-enriched Colonocyte
DistCol-enriched Colonocyte
Fraction of all cells
Young
Old
Cecum ProxCol DistCol
G
Goblet_YvO
EIF2 Signaling
Regulation of eIF4 and p70S6K Signaling
mTOR Signaling
Oxidative Phosphorylation
-log(p-value)
Cecum_Goblet
Role of PKR in Interferon Induction and Antiviral Response
ProxCol_Goblet
BAG2 Signaling Pathway
DistCol_Goblet
SPINK1 General Cancer Pathway
positive z-score
z-score = 0
negative z-score
no activity pattern available
H
Goblet_YvO
MLXIPL
MYC
STK11
AGT
IL4
IL10RA
RICTOR
Activation z-score
Cecum_Goblet
MYCL
HSF1
OGA
FAAH
SOX2
ProxCol_Goblet
TP53
MAP4K4
CEBPB
NFE2L2
DistCol_Goblet
MEF2C
MKNK1
I
Cecum
ProxCol
DistCol
Dnah5
Plac8
B3galt2
Tm4sf1
Sycn
Krt18
Lgals3
Hck
Ccnj
J
Tuft-Enteroendocrine_YvO
EIF2 Signaling
Regulation of eIF4 and p70S6K Signaling
mTOR Signaling
Cell Cycle: G1/S Checkpoint Regulation
-log(p-value)
K
Tuft-Enteroendocrine_YvO
MYC
MLXIPL
RICTOR
Activation z-score

Figure S2. Differences between compartments and during aging in different epithelial cell types, related to Fig.2, Fig.3 and Fig.4.
(A) FACS gating of Lgr5-GFP cells. **(B)** Enriched Canonical Pathways and Predicted Upstream regulators from IPA for the Stem-TA cluster. (n = 5 young, 6 old biologically independent animals) **(C)** Separate tSNE of colonocytes_1 and _2 with compartments overlaid (left) and Graph-based re-clustered colonocytes overlaid on the original tSNE (right). (n = 5 young, 6 old biologically independent animals) **(D)** Fractions of compartment-enriched colonocytes in the corresponding compartments (n = 5 young, 6 old biologically independent animals). **(E)** Top 10 marker gene heatmap for re-clustered colonocytes (n = 5 young, 6 old biologically independent animals). **(F)** Bar charts of re-clustered colonocyte fractions in different compartments in young and old. (n = 5 young, 6 old biologically independent animals; 1-tailed unpaired *t*-test; mean + SD). **(G)** Enriched Canonical Pathways from IPA for goblet cells (n = 5 young, 6 old biologically independent animals). **(H)** Predicted Upstream Regulators from IPA for goblet cells. (n = 5 young, 6 old biologically independent animals) **(I)** Top 10 marker gene heatmap for tuft cells in different compartments (n = 5 young, 6 old biologically independent animals). **(J)** Enriched Canonical Pathways from IPA for Tuft-EE cells. (n = 5 young, 6 old biologically independent animals) **(K)** Predicted Upstream Regulators from IPA for Tuft-EE cells. (n = 5 young, 6 old biologically independent animals) ns, $p>=0.05$; *, $p<0.05$; **, $p<0.01$; ***, $p<0.001$;

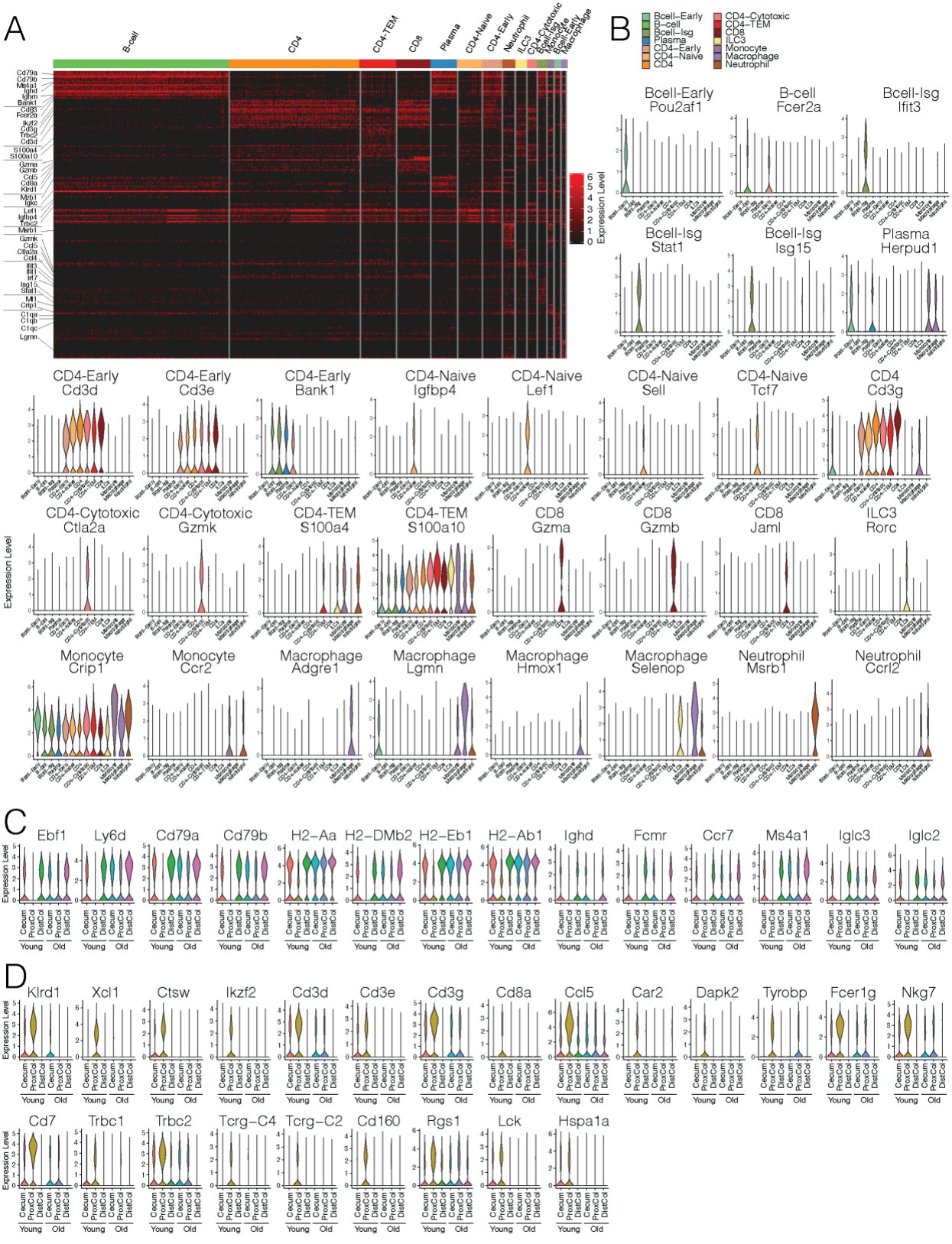
A
B-cell
CD4
CD4-TEM
CD8
Plasma
CD4-Naive
CD4-Early
Neutrophil
ILC3
CD4-Cytotoxic
Bcell-Isg
Monocyte
Bcell-Early
Macrophage
Cd79a
Cd79b
Ms4a1
Ighd
Iglmn
Bank1
Cd83
Fcer2a
Ikzf2
Cd8g
Trbc2
Cd3d
S100a4
S100a10
Gzma
Gzmb
Ccl5
Cd8a
Klrd1
Mzb1
Iglc
Lef1
Igfbp4
Trbc1
Marb1
Gzmk
Ccl5
Ctla2a
Cd4
Ifit3
Irf7
Isg15
Stat1
Mt1
Crip1
C1qa
C1qb
C1qc
Lgmn
6
5
4
3
2
1
0
Expression Level
B
Bcell-Early
B-cell
Bcell-Isg
Plasma
CD4–Early
CD4–Naive
CD4
CD4–Cytotoxic
CD4–TEM
CD8
ILC3
Monocyte
Macrophage
Neutrophil
Bcell-Early
Pou2af1
B-cell
Fcer2a
Bcell-Isg
Ifit3
Bcell-Isg
Stat1
Bcell-Isg
Isg15
Plasma
Herpud1
CD4-Early
Cd3d
CD4-Early
Cd3e
CD4-Early
Bank1
CD4-Naive
Igfbp4
CD4-Naive
Lef1
CD4-Naive
Sell
CD4-Naive
Tcf7
CD4
Cd3g
CD4-Cytotoxic
Ctla2a
CD4-Cytotoxic
Gzmk
CD4-TEM
S100a4
CD4-TEM
S100a10
CD8
Gzma
CD8
Gzmb
CD8
Jaml
ILC3
Rorc
Expression Level
Monocyte
Crip1
Monocyte
Ccr2
Macrophage
Adgre1
Macrophage
Lgmn
Macrophage
Hmox1
Macrophage
Selenop
Neutrophil
Msrb1
Neutrophil
Ccrl2
C
Ebf1
Ly6d
Cd79a
Cd79b
H2–Aa
H2–DMb2
H2–Eb1
H2–Ab1
Ighd
Fcmr
Ccr7
Ms4a1
Iglc3
Iglc2
Expression Level
Cecum
ProxCol
DistCol
Young
Old
D
Klrd1
Xcl1
Ctsw
Ikzf2
Cd3d
Cd3e
Cd3g
Cd8a
Ccl5
Car2
Dapk2
Tyrobp
Fcer1g
Nkg7
Cd7
Trbc1
Trbc2
Tcrg–C4
Tcrg–C2
Cd160
Rgs1
Lck
Hspa1a
Expression Level
Cecum
ProxCol
DistCol
Young
Old

Figure S3. Immune cell population enrichment in different compartments of young mouse colon. Related to Fig.5.

(A) Hierarchical clustering and heatmap of the expression of the top 20 markers of each of the 14 clusters in immune scRNAseq analysis (n = 4 young, 4 old biologically independent animals). **(B)** Violin plot of the expression level of typical marker genes in the same dataset as in (A) (n = 4 young, 4 old biologically independent animals). **(C)** Violin plots of the expression levels of marker genes for B-, CD4 and CD8 cells in different compartments in the large intestine of young and old mice. (n = 4 young, 4 old biologically independent animals).

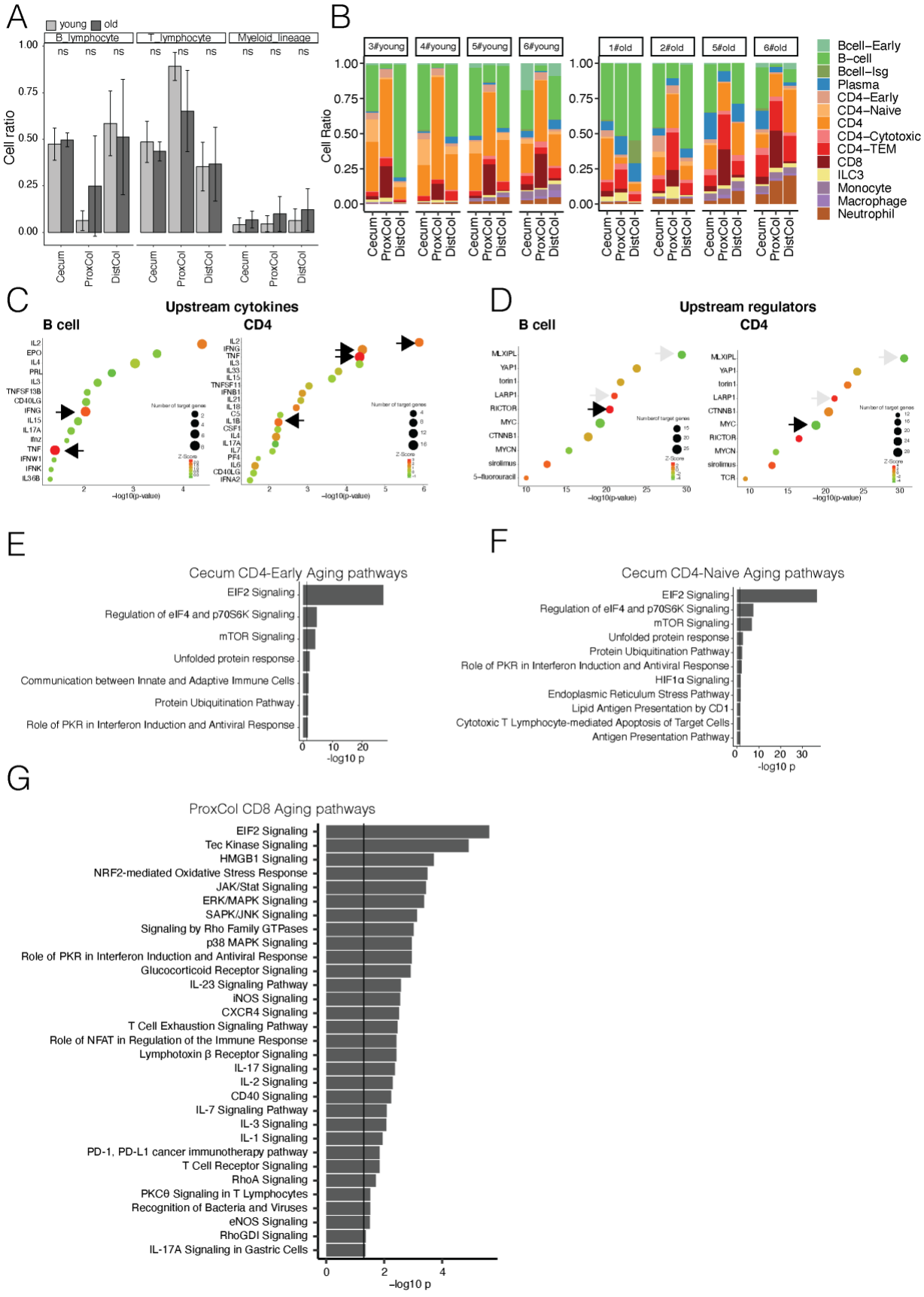
A
young
old
B_lymphocyte
T_lymphocyte
Myeloid_lineage
Cell ratio
Cecum
ProxCol
DistCol
B
3#young
4#young
5#young
6#young
1#old
2#old
5#old
6#old
Cell Ratio
Bcell−Early
B−cell
Bcell−Isg
Plasma
CD4−Early
CD4−Naive
CD4
CD4−Cytotoxic
CD4−TEM
CD8
ILC3
Monocyte
Macrophage
Neutrophil
C
Upstream cytokines
B cell
CD4
−log10(p-value)
Number of target genes
Z-Score
D
Upstream regulators
B cell
CD4
MLXIPL
YAP1
torin1
LARP1
RICTOR
MYC
CTNNB1
MYCN
sirolimus
5−fluorouracil
TCR
E
Cecum CD4-Early Aging pathways
EIF2 Signaling
Regulation of eIF4 and p70S6K Signaling
mTOR Signaling
Unfolded protein response
Communication between Innate and Adaptive Immune Cells
Protein Ubiquitination Pathway
Role of PKR in Interferon Induction and Antiviral Response
-log10 p
F
Cecum CD4-Naive Aging pathways
EIF2 Signaling
Regulation of eIF4 and p70S6K Signaling
mTOR Signaling
Unfolded protein response
Protein Ubiquitination Pathway
Role of PKR in Interferon Induction and Antiviral Response
HIF1α Signaling
Endoplasmic Reticulum Stress Pathway
Lipid Antigen Presentation by CD1
Cytotoxic T Lymphocyte-mediated Apoptosis of Target Cells
Antigen Presentation Pathway
-log10 p
G
ProxCol CD8 Aging pathways
EIF2 Signaling
Tec Kinase Signaling
HMGB1 Signaling
NRF2-mediated Oxidative Stress Response
JAK/Stat Signaling
ERK/MAPK Signaling
SAPK/JNK Signaling
Signaling by Rho Family GTPases
p38 MAPK Signaling
Role of PKR in Interferon Induction and Antiviral Response
Glucocorticoid Receptor Signaling
IL-23 Signaling Pathway
iNOS Signaling
CXCR4 Signaling
T Cell Exhaustion Signaling Pathway
Role of NFAT in Regulation of the Immune Response
Lymphotoxin β Receptor Signaling
IL-17 Signaling
IL-2 Signaling
CD40 Signaling
IL-7 Signaling Pathway
IL-3 Signaling
IL-1 Signaling
PD-1, PD-L1 cancer immunotherapy pathway
T Cell Receptor Signaling
RhoA Signaling
PKCθ Signaling in T Lymphocytes
Recognition of Bacteria and Viruses
eNOS Signaling
RhoGDI Signaling
IL-17A Signaling in Gastric Cells
−log10 p

Figure S4. Different aging characteristics of immune cells from different compartments of large intestine, related to Fig.6.

(A) Bar charts of cell ratio of the three immune lineages between young and old mice in cecum, proximal colon and distal colon. (n = 4 young, 4 old biologically independent animals; Welch's two-tailed *t*-test; mean ± SD). **(B)** Stacked bar charts showing the cell population composition in each compartment of each sample (n = 4 young, 4 old biologically independent animals). **(C, D)** Bubble plots showing typical upstream cytokines **(C)** and upstream regulators **(D)** potentially inducing the aging changes in B- and CD4 cells of large intestine. P value was calculated by using Fisher's Exact Test, z-score was calculated here to show the activated prediction (z>0) or inhibited prediction (z<0) (n = 4 young, 4 old biologically independent animals)**. (E, F, G)** Bar chart showing the -log10 enrichment p-value (x-axis) of the GO pathways enriched in cecum B cell aging **(E)**, cecum CD4-Naïve cell aging **(F)** and ProxCol CD8 aging **(G)**. P-value is calculated by the right-tailed Fisher Exact Test. (n = 4 young, 4 old biologically independent animals) ns, p>=0.05; *, p<0.05; **, p<0.01; ***, p<0.001;

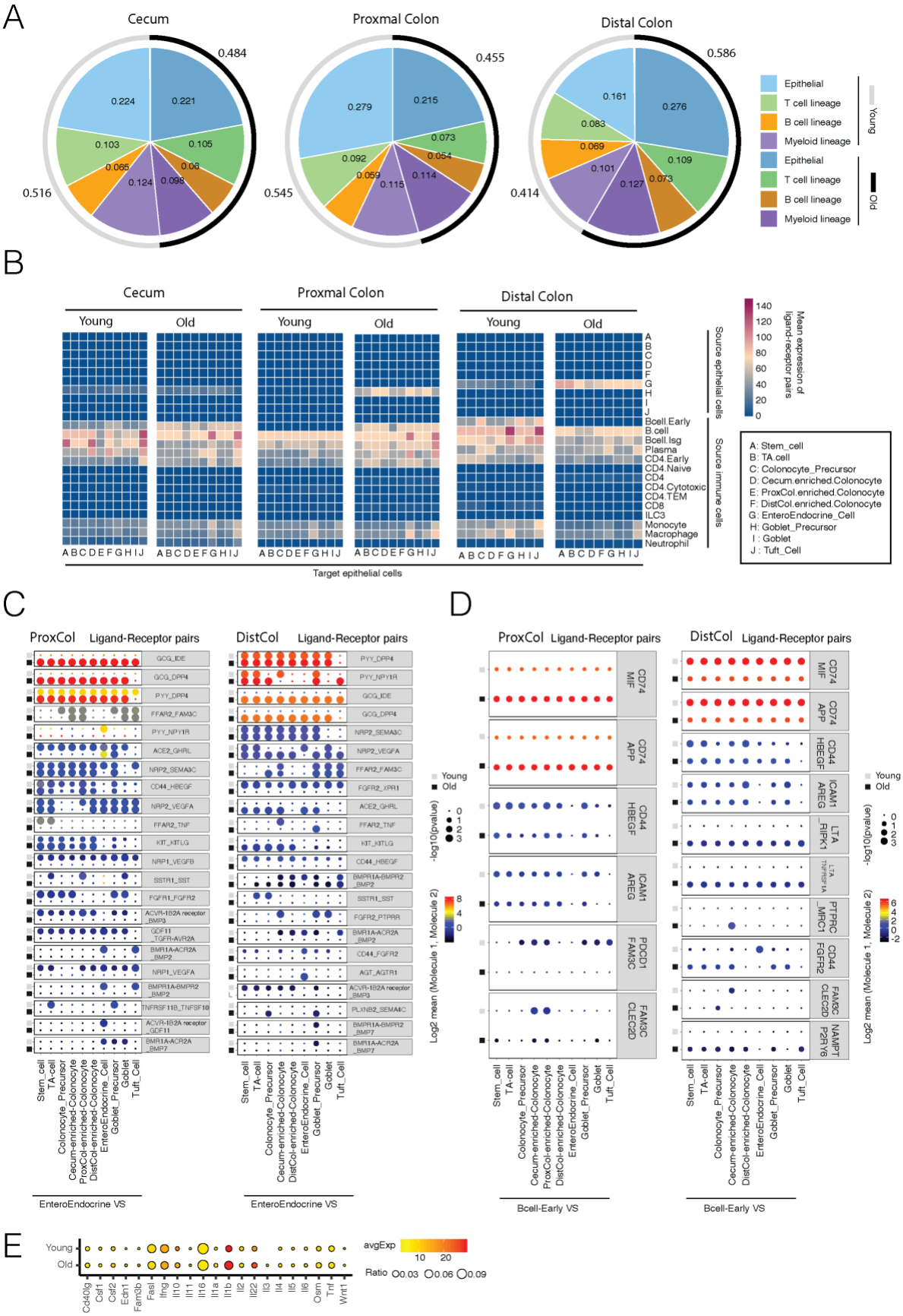
A
Cecum
Proxmal Colon
Distal Colon
0.484
0.516
0.455
0.545
0.586
0.414
Epithelial
T cell lineage
B cell lineage
Myeloid lineage
Young
Old
B
Target epithelial cells
Source epithelial cells
Source immune cells
Mean expression of ligand-receptor pairs
A: Stem_cell
B: TA.cell
C: Colonocyte_Precursor
D: Cecum.enriched.Colonocyte
E: ProxCol.enriched.Colonocyte
F: DistCol.enriched.Colonocyte
G: EnteroEndocrine_Cell
H: Goblet_Precursor
I : Goblet
J : Tuft_Cell
C
ProxCol Ligand-Receptor pairs
DistCol Ligand-Receptor pairs
EnteroEndocrine VS
D
Bcell-Early VS
-log10(pvalue)
Log2 mean (Molecule 1, Molecule 2)
E
avgExp
Ratio

Figure S5. Changes in cell-type interaction during aging, associated with interaction between immune and epithelial cells, related to Fig.7.
(A) Pie charts indicating the percentage of interacting partners between epithelial/immune cells and epithelial cells in young and old groups from cecum (left), proximal colon (middle) and distal colon (right) (n = 4 young, 4 old biologically independent animals). **(B)** Heatmap of mean expression level of ligand-receptor pairs in the interaction between epithelial/immune cells and epithelial cells in cecum (left), proximal colon (middle) and distal colon (right). Row – source cell types, column - target cell types (n = 4 young, 4 old biologically independent animals). **(C, D)** Bubble plots of significantly ($p<0.05$) interacting partners between EE cells **(C)**, B-cell-Early **(D)** and epithelial cells in proximal colon (left) and distal colon (right) (n = 4 young, 4 old biologically independent animals; P-value (rank-sum test) refers to the enrichment of the interacting ligand-receptor pair in each of the interacting pairs of cell types. First gene: ligand, second gene: receptor). **(E)** Bubble plot of expression of cytokines in young and old immune cells, that are predicted to induce epithelial aging in cecum and colon (n = 4 young, 4 old biologically independent animals).